Available online at www.sciencedirect.com

ScienceDirect

Energy Procedia 51 (2014) 109 – 118

Energy Procedia

7th Trondheim CCS Conference, TCCS-7, June 5-6 2013, Trondheim, Norway

Liquefaction of oxyfuel flue gases – Experimental results and modeling of heat transfer coefficients for pure CO_2

T. Küster[a]*, R. Eggers[a]

[a]HamburgUniversity of Technology, Eißendorfer Straße 38, 21073 Hamburg

Abstract

In this paper heat transfer coefficients for film condensation of carbon dioxide under elevated pressures are presented. The examined pressure ranges from 16-30 bars with a constant mass flow of 12 kg/h CO_2. Therefore, a pilot plant for cryogenic liquefaction of CO_2 has been built. In the installed tube in tube condenser cooling media temperatures from -25 °C to -45 °C were used. During the experiment heat transfer coefficients between 4500 and 13000 W/(m^2K) were determined. Afterwards the experimental data were compared to common correlations for film condensation. The aim was to prove whether the influence of the elevated pressure can be predicted. Finally, all correlations could predict the heat transfer under elevated pressures in a suitable manner, concerning the uncertainties in modeling and determination of heat transfer coefficients. Nevertheless not all correlations could predict the influence of elevated pressures equally well.

Selection and peer-review under responsibility of SINTEF Energi AS

Keywords: CCS; Oxyfuel; CO_2 Liquefaction; Heat Transfer

1. Introduction

In context of the joint research project ADECOS 3 the flue gas treatment of coal-fired power plants with oxyfuel adaption is examined. The investigated process is an oxyfuel power plant process with cryogenic air separation for oxygen supply and partial condensation to capture CO_2 from the flue gas.

* Corresponding author. Tel.: +49-40-42878-2133; fax: +49-40-42878-2859.
E-mail address: thorsten.kuester@tuhh.de

Selection and peer-review under responsibility of SINTEF Energi AS
doi:10.1016/j.egypro.2014.07.012

Nomenclature

Δh_V	enthalpy of evaporation	K	correction factor
A_C	system parameter	L	length
a	shear stress to gravity ratio	$\dot{m}$	mass flow
d	diameter	Nu	Nusselt number
f	film coefficient	p	pressure
F	flow coefficient	Pr	Prandtl number
g	acceleration due to gravity	Re	Reynolds number
$\dot{G}$	total mass flux (liquid + vapour)	T	temperature
h	hydraulic	u	velocity
J	dimensionless vapour velocity	z	vapour quality
k	over all heat transfer coefficient	Z	correlation parameter

Greek letters

α	heat transfer coefficient	ξ	coefficient of resistance
δ	film thickness	ρ	density
η	viscosity	τ	shear stress
λ	thermal conductivity		

Subscripts

cm	cooling media	o	outer
e	empty tube	ph	interfacial area / film surface
exp	experimental	r	reduced
film	liquid condensate phase	rel	relative
GT	assuming all mass flowing as gas	s	saturation
i	inner	tur	turbulent flow
LT	assuming all mass flowing as liquid	v	vapour
LS	assuming liquid phase flowing alone in the tube	tur	turbulent flow
		w	wall
lam	laminar flow	wav	waviness
log	logarithmic	x	local
m	mean value		

Superscripts

*	moving vapour considered	-	averaged value

The aim of the examined sub-project of ADECOS 3 is to determine the influences of oxygen purity from the air separation unit (ASU), firing, air ingress, conventional flue gas treatment, dehydration, liquefaction and distillation on the purity of the separated carbon dioxide. Therefore, the adsorptive dehydration of the process gas after compression, the heat transfer during partial condensation and the compositions of liquid and vapour phase (VLE) after liquefaction are examined.

This article presents the determination and modelling of heat transfer coefficients during film condensation of CO_2 under elevated pressures. Available correlations are mostly based on measurements under low pressure. By increasing pressure the density of the vapour phase is increased as well and hence the vapour velocity decreases. The vapour velocity again is essential for shear force impact on the film surface. This influence is explicitly considered by HADLEY's [1] approach used in the current correlation of the VDI-Wärmeatlas [2]. In addition the surface tension between liquid film and vapour phase decreases with pressure. Thus the form keeping force for the falling film is lowered. Further on increased pressures lead to higher temperature gradients between vapour and cooling media. Consequently the liquefaction rate is increased and thereby the film thickness. This leads to a higher heat conduction resistance in the film. Therefore, the heat transfer coefficient for film condensation of CO_2 under elevated pressures, between 18 and 30 bars, is determined in this work. The experimental heat transfer coefficient

is determined by an experimental liquefaction plant via energy balances. Afterwards the experimental results are compared to suitable, existing correlations, to prove whether the partial film condensation of CO_2 under elevated pressures can be represented by these mathematical models.

2. Theoretical background

For the calculation of heat transfer coefficients for film condensation many correlations have been published. Most of them use power functions based on experimental data. These empiric correlations are only suitable in the experimentally studied area. Hence the range of conditions, where the correlations are valid, is quite small. Further on the studied fluids are mainly water, various refrigerants and alcohols.

2.1. VDI Wärmeatlas, 2013

The correlation in the VDI-Wärmeatlas [2] is based on a multi-layer approach for the characterization of film condensation. Therefore, the film is divided into a near-wall and an interfacial area, taking account of the shear stress between vapour and liquid phase. In Table 1 the ranges of validity are listed.

Table 1: Ranges of validity for the heat transfer correlation from VDI-Wärmeatlas [2]

Parameter	Range of validity
Pr_{film}	$0.5 < Pr_{film} < 500$
Re_{film}	$Re_{film} < 10{,}000$
η_{film}/η_w	$0.2 < \eta_{film}/\eta_w < 5$

In the laminar flow pattern the local Nusselt number for still vapour is calculated from [3]:

$$Nu_{film,x,lam} = 0.693 \left(\frac{1 - \rho_v/\rho_{film}}{Re_{film,x}} \right)^{1/3} f_{wav} \tag{1}$$

All thermophysical properties in equation (1) are calculated at boiling temperature. The surface characteristic of the laminar film flow is taken into account by the waviness coefficient f_{wav}. For this coefficient the following approach is applied [4]:

$$f_{wav} = \begin{cases} 1 & for\ Re_{film,x} < 1 \\ Re_{film}^{0.04} & for\ Re_{film,x} \geq 1 \end{cases} \tag{2}$$

In the turbulent flow pattern the local Nusselt number is calculated according to [5]:

$$Nu_{film,x,tur} = \frac{0.0283 Re_{film,x}^{7/24} Pr_{film}^{1/3}}{1 + 9{,}66 Re_{film,x}^{-3/8} Pr_{film}^{-1/6}} \tag{3}$$

The effect of vapour shear stress on the film in moving vapours is taken into account by two corrective factors. This influence is of particular interest in compressed systems, since vapour density and friction are significantly depending on pressure. In this approach the wall and surface area are treated separately. The shear stress influence

on the wall area for both laminar and turbulent flow is considered by the factor K_w:

$$K_w = (1 + \tau_v^*)^{1/3} \tag{4}$$

At film surface the effect of shear stress is calculated separately for laminar ($K_{ph,lam}$) and turbulent ($K_{ph,tur}$) flow:

$$K_{ph,lam} = 1 + \left(Pr_{film}^{0.56} - 1\right) tanh(\tau_v^*) \tag{5}$$

$$K_{ph,tur} = 1 + \left(Pr_{film}^{0.08} - 1\right) tanh(\tau_v^*) \tag{6}$$

This leads to the approach for local Nusselt numbers for moving vapours:

$$Nu_{film,x}^* = \sqrt{\left(K_w K_{ph,lam} Nu_{film,x,lam}\right)^2 + \left(K_w K_{ph,tur} Nu_{film,x,tur}\right)^2} \tag{7}$$

The coefficient τ_v^* in the equations (4), (5) and (6) is defined as the dimensionless shear stress:

$$\tau_v^* = \frac{\tau}{\rho_{film} g \delta_{film}^+} \quad with \quad \tau = \frac{\xi}{8} \rho_v \bar{u}_{rel}^2 \tag{8}$$

The dimensionless shear stress τ_v^* is determined by the dimensionless shear stress τ_e^*, the vapour would have in an empty tube. Here the coefficient of resistance ξ is defined as follows:

$$\xi_e = 0.184 Re_{rel}^{-0.2} \quad with \quad Re_{rel} = \frac{\rho d_h \bar{u}_{rel}}{\eta} \tag{9}$$

By means of τ_e^* the dimensionless shear stress for the rough film surface then is calculated iteratively by:

$$\tau_v^* = \tau_e^* \left(1 + 550 F (\tau_v^*)^{a^*}\right) \tag{10}$$

Thereby F is defined as a flow coefficient including the Reynolds number for relative vapour liquid velocities,

$$F = \frac{max\left[\left(2Re_{film,x}\right)^{0.5}; 0.132 Re_{film}^{0.9}\right]}{Re_{rel}^{0.9}} \frac{\eta_{film}}{\eta_v} \sqrt{\frac{\rho_v}{\rho_{film}}} \tag{11}$$

and the coefficient a^* as the relationship between shear stress and gravity of the film.

$$a^* = \begin{cases} 0.3 & for \ \tau_v^* \geq 1 \\ Re_{film}^{0.04} & for \ \tau_v^* < 1 \end{cases} \tag{12}$$

The last variable δ^+ the film thickness is calculated by means of the flow coefficient as well:

$$\frac{\delta^+}{d} = \frac{6.59F}{\sqrt{1+1400F}} \tag{13}$$

2.2. Shah, 2009

In 2009 SHAH [6, 7] published an improved and extended version of his correlation for heat transfer during condensation in horizontal, vertical and downward-inclined tubes. This correlation is validated for a wide range of properties and flow patterns:

Table 2: Ranges of validity for the heat transfer correlation by SHAH

Parameter	Range of validity
p_r	$0.0008 < p_r < 0.9$
Pr_{film}	$1 < Pr_{film} < 18$
Re_{LT}	$68 < Re_{LT} < 84827$
Re_{GT}	$9534 < Re_{GT} < 523317$
Z	$0.005 < Z < 20$
J_v	$0.06 < J_v < 20$
z_v	$0.01 < z_v < 0.99$

For vertical tubes SHAH defined three heat transfer regimes, a laminar regime, a transition area and a turbulent regime:

$$regime = \begin{cases} laminar & J_v \leq 0.89 - 0.93exp(-0.087Z^{-1.17}) \\ turbulent & J_v \geq 1/(2.4Z + 0.73) \end{cases} \tag{14}$$

Where the dimensionless vapour velocity is defined as:

$$J_v = \frac{z_v \dot{G}}{\left(g d_i \rho_v (\rho_{film} - \rho_v)\right)^{0.5}} \tag{15}$$

SHAH's correlating parameter Z is given by:

$$Z = \left(\frac{1}{z_v - 1}\right)^{0.8} {p_r}^{0.4} \tag{16}$$

The heat transfer correlation for laminar film condensation in vertical tubes is given in equation (17). It is the Nusselt equation with a constant increased by 20% as recommended by MCAdams [8].

$$\alpha_{film,x,lam} = 1.32 Re_{LS}^{-1/3} \left(\frac{\rho_{film}(\rho_{film} - \rho_v) g \lambda_{film}^3}{\eta_v^2}\right)^{0.8} {p_r}^{0.4} \tag{17}$$

With the exponent $n=0.0058+0.557p_r$ the heat transfer coefficient for the turbulent regime is calculated by:

$$\alpha_{film,x,tur} = Nu_{LT,x}\left(\frac{\eta_{film}}{14\eta_v}\right)^n\left[(1-z_v)^{0.8}+\frac{3.8z_v^{0.76}(1-z_v)^{0.04}}{Pr^{0.38}}\right]\frac{\lambda_{film}}{d_i} \tag{18}$$

The term $Nu_{LT,x}$ is given by the Dittus-Boelter equation:

$$Nu_{LT,x} = 0.023Re_{LT,x}^{0.8}Pr_{film}^{0.4} \tag{19}$$

The transition area between laminar and turbulent flow is calculated by the addition of equation (17) and (18):

$$\alpha_{film,x,lam-tur} = \alpha_{film,x,lam} + \alpha_{film,x,tur} \tag{20}$$

2.3. Chen, 1987

Another correlation for heat transfer during film condensation in vertical tubes was published by CHEN [9] in 1987. The correlation is also fitted on experimental data. However there is no range of validity given. The influence of the moving fluid is taken into account by an approach for the dimensionless shear stress τ^*_{Chen} (21). This formulation was established by Dukler and is based on experimental data for adiabatic two-phase annular cocurrent downward flow of gas and liquid.

$$\tau^*_{Chen} = A_C\left(Re_{LT}-Re_{film,x}\right)^{1.4}Re_{film,x}^{0.4} \quad with \quad A_C = \frac{0.252\lambda_{film}^{1.177}\lambda_v^{0.156}}{d_i^2 g^{2/3}\rho_{film}^{0.553}\rho_v^{0.78}} \tag{21}$$

With A_C as a system parameter the local heat transfer coefficient is given by:

$$Nu_{film,x} = \left(\left(0.31Re_{film}^{-1.32}+\frac{Re_{film,x}^{2.4}Pr^{3.9}}{2.37\cdot 10^{14}}\right)^{1/3}+\frac{Pr^{1.3}A_C}{771.6}\left(Re_{LT}-Re_{film,x}\right)^{1.4}Re_{film,x}^{0.4}\right)^{0.5} \tag{22}$$

3. Materials and methods

3.1. Liquefaction Pilot Plant

For the experimental studies a pilot plant for cryogenic CO_2-liquefaction has been built. The plant consists of four main components: the compressor, the condenser, the expansion valve and the evaporator (Figure 1). The piston compressor works oil-less and enables pressures up to 80 bars. Downstream the compression the total gas flow is determined via a coriolis mass flow meter and cooled down to saturation temperature, corresponding to the pressure, before it enters the condenser. After partial condensation the two-phase stream is separated and the masses of the liquid and the vapour phases are measured by coriolis mass flow meters as well. Afterwards the streams are mixed, expanded, evaporated and recycled to the compressor.

The heat transfer coefficient is determined by the amount of liquefied gas, measured after the phase separator. Therefore, the level in the 3.8 L phase separator is kept constant by means of a manually operated low flow metering valve. The level is observed via a high pressure view cell, installed by the principle of communicating vessels, over 15 minutes with a maximum deviation of 0.05 kg/h. Phase separator and mass flow meters, downstream the condenser, are well isolated and installed in an isolated and tempered chamber. This setup leads to

a precise determination of the liquefied mass flow. The measurement and control of the plant is realized by a programmable logic controller (PLC).

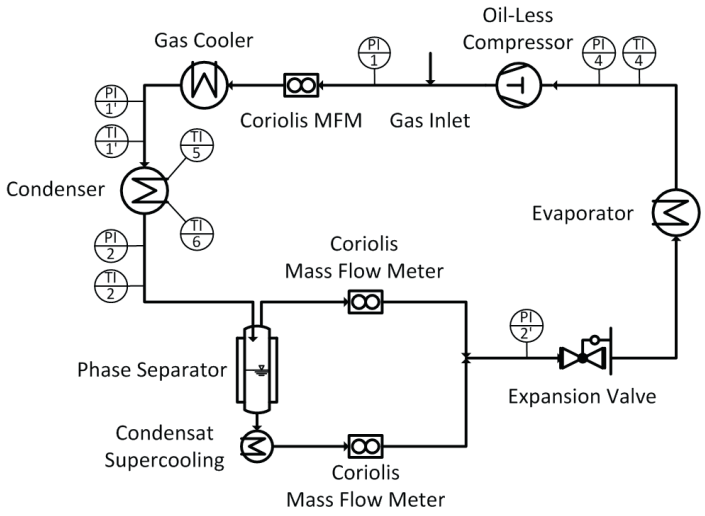

Figure 1: Simplified piping and instrumentation diagram of the liquefaction pilot plant

3.2. Experimental determination of heat transfer coefficients

The mean experimental heat transfer $\alpha_{m,film,exp}$ is determined by an energy balance. Assuming no energy input from the environment, the whole enthalpy of evaporation is transferred from CO_2 to cooling media. The total energy balance for the condenser with the length L and the logarithmic temperature difference is then given by:

$$k_m A(T_s - T_{cm})_{log} = \Delta h_V \dot{M}_{film} \tag{23}$$

where:

$$\frac{1}{k_m A} = \frac{1}{\pi L}\left(\frac{1}{\alpha_{m,film,exp} d_i} + \frac{ln\left(\frac{d_o}{d_i}\right)}{2\lambda_{m,tube}} + \frac{1}{\alpha_{m,cm} d_o}\right) \tag{24}$$

leads to:

$$\alpha_{m,film,exp} = \left[d_i\left(\frac{\pi L(T_s - T_{cm})_{log}}{\Delta h_V \dot{m}_{film}} - \frac{1}{\alpha_{m,cm} d_o} - \frac{ln\left(\frac{d_o}{d_i}\right)}{2\lambda_{m,tube}}\right)\right]^{-1} \tag{25}$$

In equation (25) it is assumed that the boiling temperature is constant. This assumption is justified by the small pressure drop over the condenser of maximum 0.9 bars. This pressure drop leads to a difference in saturation temperatures of 0.89 K using a ΔT_{log} of minimum 9.85 K. Fluid properties are calculated on the basis of VDI-Wärmeatlas [2]. Systematic and random errors are taken into account by propagation of uncertainties with a coverage factor of $k = 2$. The systematic measurement uncertainties are listed in Table 3.

Table 3: Systematic uncertainties of the input values

Input value	Measurement uncertainty
Temperature	± (0.3+0.005T(°C))
Pressure	± 0.5 %
Mass flow condensate	± 0.05 kg/h
Mass flow cooling media	± 0.1 l/min
Condenser length	± 0.5 mm
Heat conductivity tube material	± 0.5 W/(m K)

4. Experimental Results

4.1. Condensate mass flow

Figure 2 shows the measured condensate streams as a function of pressure for different cooling media temperatures between -25 °C and -45 °C. With increasing pressure the amount of liquefied CO_2 rises almost linearly. This originates from the decreasing heat of evaporation and the increasing saturation temperature of CO_2. As a consequence more heat can be transferred due to the higher temperature gradient between cooling media and film surface. Further on a decrease of cooling media temperature by 5 K leads to an improved liquefaction of about 1 kg/h. This fact is also attributed to the increased temperature gradient. Generally the condensate mass flows can be reproduced reliably in a range of 1.9 to 6.8 kg/h with an accuracy of 0.05 kg/h. The deviations lie within the measurement uncertainty of the coriolis mass flow meter and are considered to be negligibly low.

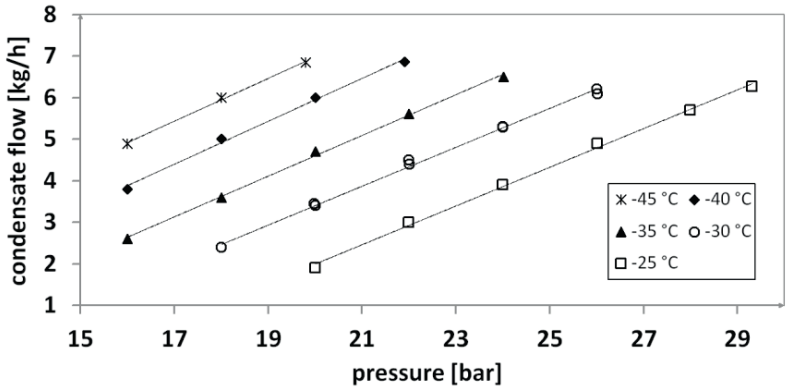

Figure 2: Liquefied CO_2 as function of pressure for different cooling media temperatures, $\dot{m}_{CO_2}$=12 kg/h, Tube in tube heat exchanger (outer tube: d_o=18 mm, d_i=15 mm | inner tube: d_o=6 mm, d_i=4 mm)

4.2. Experimental heat transfer

The determined heat transfer coefficients for all cooling media temperatures are shown in Figure 3. Values between 4500 and 13000 W/(m^2K) have been observed for pressures from 18 to 30 bars using constant flow rates of 12 kg/h CO_2. The figure shows a decreasing heat transfer coefficient with increasing pressure. An explanation is the lower velocity of the vapour phase due to higher densities at higher pressures. From 16 - 30 bars the vapour velocity decreases by 49%. Thus, the Reynolds numbers decreases from $8.5x10^4$ to $7.9x10^4$. Nevertheless the vapour flow is still turbulent even at high pressures.

Further on the heat transfer is depending on the shear stress between vapour and film surface as mentioned in chapter 2. The shear forces at the surface are depending on the vapour velocity as well. Equation (8) shows a quadratic relationship. As a consequence the shear stress decreases with increasing pressure. This leads to a lower heat transfer since the film thickness increases and hence the thermal conduction resistance. Moreover the film surface is less turbulent and therefore the temperature gradient in the near-surface area is smaller.

The error bars in Figure 3 show an increasing uncertainty with decreasing pressure. This effect can be explained by the low liquefaction rate at low pressures (cf. Figure 2). As a consequence the impact of systematic and random errors on the heat transfer coefficients is higher in this area.

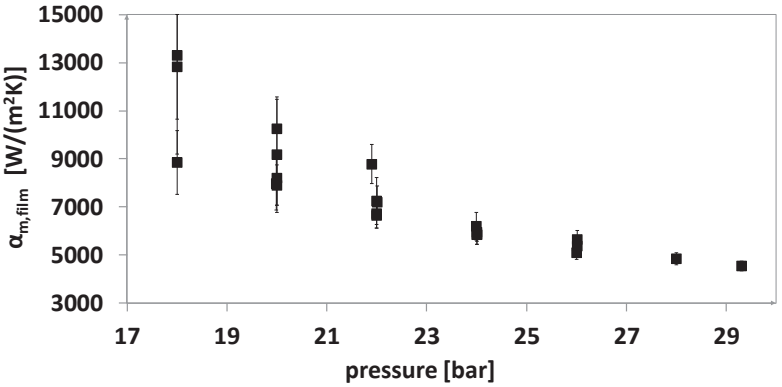

Figure 3: Mean heat transfer coefficients as function of pressure, $\dot{m}_{CO_2}$=12 kg/h, Tube in tube heat exchanger (outer tube: d_o=18 mm, d_i=15 mm | inner tube: d_o=6 mm, d_i=4 mm)

4.3. Comparison between Experiments and Simulations

In figure 4 the experimental results are compared to the values calculated according to the models introduced in chapter 2 in order to prove, weather the heat transfer for film condensation of CO_2 at elevated pressures can be predicted accurately. Figure 4 shows the values for two different series of measurement at -25 °C and -30 °C cooling media temperature. Both diagrams show that the heat transfer for film condensation of CO_2 under elevated pressures is predictable in general. The VDI [2] correlation overestimates the experimental values constantly by an amount of 35 % but shows the right characteristic for the pressure dependence of the heat transfer coefficient.

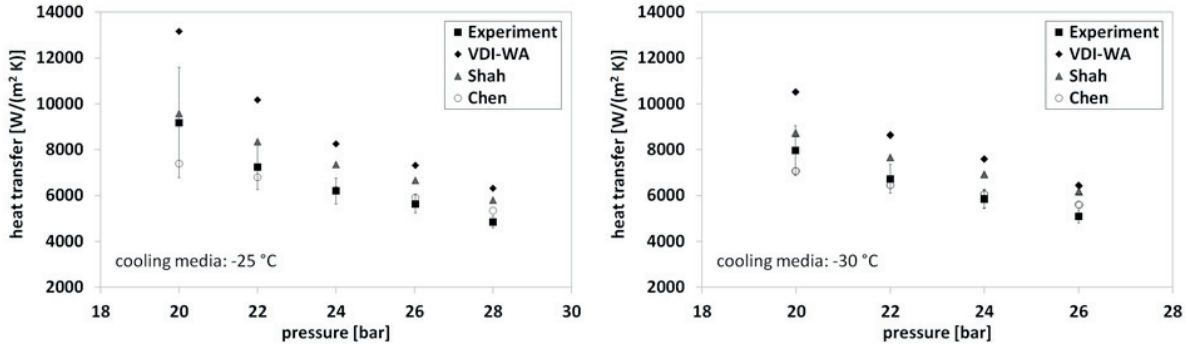

Figure 4: Experimental heat transfer compared to simulated values for different cooling media temperatures, $\dot{m}_{CO_2}$=12 kg/h, Tube in tube heat exchanger (outer tube: d_o=18 mm, d_i=15 mm | inner tube: d_o=6 mm, d_i=4 mm)

The correlation by SHAH [7] shows a smaller overestimation and a good characteristic in compliance with the experiment as well. CHEN [9] gives the lowest deviation but the curve characteristic does not fit the experimental data. This becomes particularly obvious in the lower pressure region at high vapour velocities.

5. Summary and outlook

The heat transfer for film condensation of CO_2 under elevated pressures has been examined and compared to different correlations in order to prove whether the experimental values can be predicted accurately by these approaches. The experiments have been carried out at condenser pressures between 16 and 30 bars with a constant carbon dioxide mass flow of 12 kg/h and cooling media temperatures between -25 °C and -45 °C. The determined film heat transfer coefficients lie within 4500 and 13000 W/(m^2K). All correlations predict the heat transfer in a suitable manner. The VDI-Wärmeatlas [2] correlation shows the right dependence over the examined pressure region but overestimates the experimental data by 35 % constantly. The values calculated by SHAH [7] also show a good characteristic with a smaller overestimation. CHEN [9] does not predict the influence of high vapour velocities and the related shear stress in a proper way, nevertheless the correlation gives the smallest deviation from the experimental data.

In further studies the influence of inert gases on the partial condensation will be examined. First experiments with gas mixtures have been carried out with promising results. The modelling of partial condensation by aid of the Maxwell-Stefan diffusion model is in progress.

Acknowledgements

The ADECOS 3 Project is part of the COORETEC initiative of the German Federal Ministry of Economics and Technology. The project is founded additionally by partners from industry, listed in alphabetical order: ALSTOM Carbon Capture GmbH, Babcock Borsig Steinmüller GmbH, Clyde Bergemann GmbH, EnBW Kraftwerke AG, E.ON New Build & Technology GmbH, EVN AG and Vattenfall Europe Generation AG. The author gratefully thanks all partners for the support.

References

[1] Hadley M. Kondensation binärer Dampfgemische unter dem Einfluß der vollturbulenten Gasströmung bei Drücken bis 13 bar. Dissertation, Paderborn; 1996.
[2] Verein Deutscher Ingenieure. VDI-Wärmeatlas. 11th ed. Berlin: Springer; 2013.
[3] Nußelt W. Die Oberflächenkondensation des Wasserdampfes. VDI Zeitschrift 1916; 60.
[4] Kutateladze SS, Gogonin II. Heat transfer in film condensation of slowly moving vapour. Int J Heat Mass Trans 1979; 22:12.
[5] Müller J. Wärmeübergang bei der Filmkondensation und seine Einordnung in Wärme- und Stoffübertragungsvorgänge bei Filmströmungen. VDI-Verlag; 1991.
[6] Shah MM. A general correlation for heat transfer during film condensation inside pipes. Int J Heat Mass Trans 1979; 22:4.
[7] Shah MM. An Improved and Extended General Correlation for Heat Transfer During Condensation in Plain Tubes. HVAC&R Research 2009, 15:5.
[8] MacAdams WH. Heat transmission. 3rd ed. New York: McGraw-Hill; 1954.
[9] Chen SL. General Film Condensation Correlations. Experimental Heat Transfer 1987; 1:2.